Astron. Astrophys. 325, 269–276 (1997)

ASTRONOMY
AND
ASTROPHYSICS

IR emission from carbon-dust in nebulae

Cesare Cecchi-Pestellini[1], Luigi Colangeli[1], Vito Mennella[1], Pasquale Palumbo[2], Alessandra Rotundi[2], and Ezio Bussoletti[2]

[1] Osservatorio Astronomico di Capodimonte, via Moiariello 16, I-80131 Napoli, Italy
[2] Istituto di Fisica Sperimentale, Istituto Universitario Navale, via A. De Gasperi 5, I-80133 Napoli, Italy

Received 30 July 1996 / Accepted 10 March 1997

Abstract. The relevance of dust in circumstellar emission has to be carefully considered in order to properly interpret astronomical observations. In this work we focus on carbon-rich planetary nebulae in order to produce models able to account for IR and submillimeter dust emission. The effects of dust selective absorption on the ionization structure are investigated by means of dust opacities measured in laboratory experiments. The infrared spectrum emitted by dust present in both ionized and neutral circumstellar regions is calculated for various choices of the model parameters. The IR dust continuum emission in planetary nebula NGC 7027 is also modelled on the basis of a possible evolutionary scenario for carbon dust grains. Our results provide evidence that by means of UV dust processing it is possible to account for most of the spectral distribution of carbon-rich planetary nebulae. However, non-equilibrium emission is needed to explain near-IR bands and part of the underlying continuum.

Key words: ISM: dust – ISM: planetary nebulae

1. Introduction

Circumstellar (and interstellar) dust gives rise to a number of spectral features, which present a wide spectral diversity from source to source. The problem of the nature of cosmic dust is strongly related to the possibility that all these variations can be reconciled through an evolutionary physical-chemical scheme of dust materials. We approach the problem of cosmic dust simulation by using laboratory data available for amorphous carbon (AC). AC shows continuous variations in the optical properties depending on laboratory physical processing (Mennella et al., 1996a), simulating to some extent "real" astrophysical phenomena.

Planetary (and in general gaseous) nebulae (PN) have proved to be particularly useful for determining the nature of materials responsible for the various infrared dust features and continuum. Indeed, while carbon-rich objects evolving from the asymptotic giant branch to the PN stage show large variations from source to source, C-rich PNe all show very similar IR spectra (Buss et al., 1993). Therefore, the PN environment represents a natural starting point for considering cosmic dust as an agent of the diversity of the astronomical observations in the infrared.

Carbon-rich PN environments have been widely studied. Natta and Panagia (1981) carried out an analysis of the available far-IR data for ten PNe. They assumed that dust resided only inside the ionized region. Their results appeared to imply that dust grains were being destroyed as the nebula evolved. Harrington et al. (1988) have developed a model for the dust emission from NGC 3918 using graphite and AC grains with an MRN size distribution. Hoare (1988) extended the previous model to include the emission from a circum-nebular dust shell and a mixture of mineral grains. The gas-to dust mass ratios resulting from Hoare's modelling of a few of C-rich PNe were a factor of ten smaller than those usually estimated for the interstellar medium (ISM). Barlow (1989) noted that, if the respective ratios estimated for the ISM and PNe are correct, PNe cannot contribute significantly to the interstellar dust content. This is a rather surprising result, in view of the fact that the red giant progenitors of PNe are thought to be the major source of refractory dust grains. However, recent published data on stellar composition show that carbon in the sun is substantially more abundant than in other stars (Snow and Witt, 1995). A reduction in the galactic carbon budget strongly constrains the quantity that is available for the formation of interstellar dust.

The modelling of dust emission has progressed significantly in recent years (e.g. Middlemass, 1990; Hoare et al., 1992; Zavagno and Baluteau, 1995). The modelling results have shown that AC grains could be responsible for far-IR emission in PNe. However, the carriers of mid-IR emission remain unclear.

In this work we analyse the response of AC dust to ultraviolet radiation, using dust data acquired at our own laboratory (samples ACH2,ACAR,BE; Colangeli et al., 1996). Although dust samples were obtained by condensation under different conditions, an evolutionary trend is consistent with the variations in the physical properties of the samples (cf Sect.3). Therefore, laboratory data can support a possible scenario for dust evolution in PN environments, in which UV irradiation of H-rich carbon grains modifies the optical properties of dust embedded in the ionized shell. These environmentally-induced

Send offprint requests to: C. Cecchi-Pestellini

changes are simulated adopting evolutionary-linked dust samples (ACH2 → ACAR → BE) in the neutral and ionized shells. We would like to emphasize that we are not considering a mixture of our dust samples, as usually done when adopting multimodal dust populations. Different samples are not co-extensive, since they represent different evolutionary stages of the same parental material.

In gaseous nebulae the dust and ionized gas are partially comixed in the HII region. However, the dust component, primarily responsible for the extinction, likely resides in a shell outside the volume containing the dust emitting the near-infrared thermal continuum. Although few nebulae are spherically symmetrical, and density distributions are seldom a simple function of distance from the exciting star, it is possible to construct reasonably straightforward models that are often useful in the interpretation and in the assessment of the observations. We assume that the ionizing source is located at the center of a two-shell structure. There is allowance for a central cavity devoid of both dust and gas, which is embedded in a constant density shell. An external denser neutral layer surrounds the inner shell. It is worthwhile noting that the dust associated with nebulae has been exposed to intense ultraviolet radiation and to dynamical processes.

After computing the radiation field and the nebular ionization structure using the photo-ionization model described in Sect. 2, we derive a model for the IR continuum emission of carbon dusty nebulae. The dust properties adopted are described in Sect. 3. Dust temperatures are calculated assuming thermal equilibrium at each radial point in the nebula. Thermal emission from dust is then obtained by integrating the grain emissivity over the volume of the nebula, extended to include the contribution of the neutral shell (Sect. 4). In Sect. 5 we model the IR dust continuum emission in the planetary nebula NGC 7027. Last section is devoted to a discussion of the physical consistency of the evolutionary scenario for dust grains in gaseous nebulae.

2. Ionization structure

We consider spherical, static nebulae in thermal and ionization equilibrium. Although an ionized nebula cannot exist in static equilibrium, the static assumption is quite reasonable because, in most cases, the energetics is dominated by radiation fields with negligible mechanical energy conversion into radiation. Thermal and ionization balance applies everywhere, and the only energy input is through photoionization of the gas by a time-independent source.

The central stars of nebulae (in particular of PNe) radiate energetic photons that may doubly ionize helium to produce an inner zone of He^{2+}. Since the recombination of He^{2+} to He^{+} is accompanied by the emission of photons that ionize hydrogen, we can safely assume that the gas in the inner part is fully ionized. As a consequence, all photons energetically capable of producing He^{2+} are fully absorbed in the central region. The ionization structure of the surrounding plasma can be determined by solving the ionization equations for H and He in a radiation field with frequencies lying between the ionization threshold of H, $\nu_{\rm L}$, and the ionization threshold of He^{+}, $4\nu_{\rm L}$.

It is convenient to distinguish between radiation that can ionize only hydrogen ($\nu_{\rm L} \leq \nu < 1.8\nu_{\rm L}$) and radiation capable of ionizing both hydrogen and helium ($\nu \geq 1.8\nu_{\rm L}$). We define the following average quantities, integrated over frequencies above the Lyman limit $\nu_{\rm L}$

$$\langle\sigma_{\rm H}\rangle_1 = \frac{\int_{\nu_{\rm L}}^{1.8\nu_{\rm L}} \sigma_{\rm H}(\nu) L_\nu(r) d\nu}{\int_{\nu_{\rm L}}^{1.8\nu_{\rm L}} L_\nu(r) d\nu} \tag{1a}$$

$$\langle\sigma_{\rm H}\rangle_2 = \frac{\int_{1.8\nu_{\rm L}}^{4\nu_{\rm L}} \sigma_{\rm H}(\nu) L_\nu(r) d\nu}{\int_{1.8\nu_{\rm L}}^{4\nu_{\rm L}} L_\nu(r) d\nu} \tag{1b}$$

$$\langle\sigma_{\rm He}\rangle_2 = \frac{\int_{1.8\nu_{\rm L}}^{4\nu_{\rm L}} \sigma_{\rm He}(\nu) L_\nu(r) d\nu}{\int_{1.8\nu_{\rm L}}^{4\nu_{\rm L}} L_\nu(r) d\nu} \tag{1c}$$

$$\langle\sigma_{\rm d}\rangle_1 = \frac{\int_{\nu_{\rm L}}^{1.8\nu_{\rm L}} \sigma_{\rm d}(\nu) L_\nu(r) d\nu}{\int_{\nu_{\rm L}}^{1.8\nu_{\rm L}} L_\nu(r) d\nu} \tag{1d}$$

$$\langle\sigma_{\rm d}\rangle_2 = \frac{\int_{1.8\nu_{\rm L}}^{4\nu_{\rm L}} \sigma_{\rm d}(\nu) L_\nu(r) d\nu}{\int_{1.8\nu_{\rm L}}^{4\nu_{\rm L}} L_\nu(r) d\nu} \tag{1e}$$

where L_ν is the number of photons per sec per Hz crossing a sphere of radius r with the source at its centers, $\sigma_{\rm H}(\nu)$ and $\sigma_{\rm He}(\nu)$ are the photoionization cross-sections of hydrogen and helium, respectively, and

$$\sigma_{\rm d}(\nu) = \frac{\mathscr{R}}{1.086}\left(\frac{A_\nu}{A_V}\right) \ {\rm cm}^2 \tag{2}$$

In the above expression, $\mathscr{R} = A_V/N_{\rm H}$ is the dust-to-gas ratio and A_ν/A_V is the extinction scale with respect to the visible.

As it is customarily assumed in gaseous nebula calculations, we split the radiation field into two components, the attenuated direct stellar radiation and the diffuse component. For a stellar radiation $L_s(r,\mu) = L_s(r)\delta(1-\mu)$, the angular integration yields a transfer equation

$$\frac{d}{dr} L_s^{(1)} = -n_{\rm H}\left(f_{\rm HI}\langle\sigma_{\rm H}\rangle_1 + \langle\sigma_{\rm d}\rangle_1\right) L_s^{(1)} \tag{3}$$

$$\frac{d}{dr} L_s^{(2)} = -n_{\rm H}\left(f_{\rm HI}\langle\sigma_{\rm H}\rangle_2 + Y f_{\rm HeI}\langle\sigma_{\rm He}\rangle_2 + \langle\sigma_{\rm d}\rangle_2\right) L_s^{(2)} \tag{4}$$

where $Y = n_{\rm He}/n_{\rm H}$, $f_{\rm HI}$ and $f_{\rm HeI}$ are the neutral fractions of hydrogen and helium, respectively, and

$$L_s^{(1)} = \int_{\nu_{\rm L}}^{1.8\nu_{\rm L}} L_\nu(r) d\nu \tag{5b}$$

$$L_s^{(2)} = \int_{1.8\nu_{\rm L}}^{4\nu_{\rm L}} L_\nu(r) d\nu \tag{5b}$$

There could also be two differential equations for diffuse photons. In many ionization calculations, the transfer of diffuse

radiation is by-passed by means of the introduction of an on-the-spot (OTS) approximation: the hydrogen diffuse radiation field is OTS absorbed only by hydrogen and the helium radiation field only by helium, without any transfer problem for diffuse radiation. This approximation has the great (practical) advantage that the ionization structure of a nebula is determined by a single integration step, while the complete solution would require an iterative procedure. In their early classical works, Hummer and Seaton (1963,1964) demonstrated that the ionization computed with the OTS approximation is in reasonable agreement with the exact result. Rubin (1984) confirmed the expectation that the ionization structure was adequately represented, but not the temperature distribution, particularly in the central region. This method fails when it is extended to dusty nebulae: the main inconsistency comes from dust absorption of the diffuse ionizing radiation, which is not entirely absorbed by gas. Sarazin (1977) compared OTS models with models based on the modified outward-only approximation and found some discrepancies and substantial differences in the thermal structure, as in the case of dust-free nebulae. Because the use of an OTS approximation for a dusty PN can yield inaccurate results, we use the generalized-on-the-spot (GOTS) approximation (Petrosan and Dana, 1975), which includes OTS absorption of the diffuse fields by both hydrogen and dust. Following Tielens and deJong (1979), we obtain the differential equations which govern the spatial evolution of the neutral column density of H and He, $N_{\rm HI}$ and $N_{\rm HeI}$, under the OTS approximation

$$\frac{dN_{\rm HI}}{dr} = \frac{f_{\rm e}(C_{\rm H} - p\,C_{\rm He}(1 - \frac{dN_{\rm HeI}}{dr}))}{f_{\rm e}C_{\rm H} + \langle\sigma_{\rm H}\rangle_1 L_s^{(1)} + \langle\sigma_{\rm H}\rangle_2 L_s^{(2)}} \tag{6a}$$

$$\frac{dN_{\rm HeI}}{dr} = \frac{f_{\rm e}C_{\rm He}}{f_{\rm e}C_{\rm He} + Y\langle\sigma_{\rm He}\rangle_2 L_s^{(2)}} \tag{6b}$$

where $f_{\rm e} = n_{\rm e}/n_{\rm H}$ is the fractional ionization, $C_{\rm H} = 4\pi r^2 \alpha_B({\rm H},T) n_{\rm H}$, $C_{\rm He} = 4\pi r^2 \alpha_B({\rm He},T) n_{\rm He}$, α_B is the recombination coefficient to all levels down to the 2nd, and p is the fraction of the total number of recombinations to excited levels of helium, generating hydrogen-ionizing photons. $n_{\rm e}$ is the electronic density.

Similarly, we derive the GOTS approximation equations

$$\frac{dN_{\rm HI}}{dr} = \frac{f_{\rm e}C_{\rm H}\frac{\alpha_A({\rm H,T})}{\alpha_{\rm B}({\rm H,T})}}{f_{\rm e}C_{\rm H}\frac{\alpha_A({\rm H,T})}{\alpha_{\rm B}({\rm H,T})} + \langle\sigma_{\rm H}\rangle_1 L^{(1)} + \langle\sigma_{\rm H}\rangle_2 L^{(2)}} \tag{7a}$$

$$\frac{dN_{\rm HeI}}{dr} = \frac{f_{\rm e}C_{\rm He}\frac{\alpha_A({\rm He,T})}{\alpha_{\rm B}({\rm He,T})}}{f_{\rm e}C_{\rm He}\frac{\alpha_A({\rm He,T})}{\alpha_{\rm B}({\rm He,T})} + Y\langle\sigma_{\rm He}\rangle_2 L^{(2)}} \tag{7b}$$

where $L^{(i)} = L_s^{(i)} + L_D^{(i)}$, $L_D^{(i)}$ is the diffuse field (Tielens and deJong, 1979) and α_A is the total recombination coefficient.

Dust mixed with gas can alter the structure of a nebula by reducing the volume of ionized gas. Furthermore, the frequency dependence of the dust absorption coefficient may modify the spectrum of the ionizing radiation, which in turn changes the ionization structure. The dust model around hot stars requires a knowledge of the optical constants for the grain material up to the extreme ultraviolet. Unfortunately, since there are no direct observations, our knowledge of the nature and far UV properties of dust grains is rather poor. Mathis (1985) emphasized that realistic dust cross sections behave in a rather hydrogenic fashion, making the radiation field resemble that of a hotter star. In this work, the optical properties of the dust mixture inside the double shell are those derived in the laboratory for various kinds of AC grains (Colangeli et al., 1995). The wide spectral range covered by measurements provides a set of self-consistent data (see next section) which can be applied to determine the impact of AC grains on astrophysical models.

The inclusion of dust scattering, which would substantially complicate the radiative transfer problem, has a negligible effect on the nebular structure (Mathis, 1985). Since interstellar dust is generally known to be forward scattering (Savage and Mathis, 1979), the previous equations have been stated under the implicit assumption of perfectly forward dust scattering.

The GOTS-coupled differential equations were integrated using the Bulirsh-Stoer method. At each integration step, the derivatives were obtained with a Newton-Raphson technique, using the OTS values, with some constant values for the electronic density as initial evaluations.

We characterized the stellar radiation field by its luminosity in photons capable of ionizing atomic hydrogen, $Q_{\rm H}$, and by a black-body spectral distribution at a temperature T_s with a high-frequency cutoff consistent with the selected value of $Q_{\rm H}$.

3. Laboratory experiments

The condensation techniques and boundary conditions used to produce the amorphous carbon grains considered here (BE, ACAR, ACH2 samples) have been extensively presented in previous papers (e.g. Colangeli et al. 1995), to which we refer the reader for further details. ACAR and ACH2 samples are obtained by striking an arc between amorphous carbon electrodes in argon and in H_2 atmosphere, respectively; BE grains are synthesised by burning benzene in air. In addition, thermal annealing of the ACH2 sample has demonstrated that this material evolves in optical and structural properties (Mennella et al. 1995a,b).

The morphological analysis of the samples considered here, by means of transmission (T.E.M.) and scanning (S.E.M.) electron microscopy, shows that ACAR and ACH2 grains are spheroidal with average diameter of about 10 nm. Grains are agglomerated in clusters of some 4–5 particles, which, in turn, form chain structures. The BE grains have similar properties, but the average diameter is 30 nm.

As far as the optical properties are concerned, we note that all the spectra are characterised by: a) a far UV maximum which falls off around 80–90 nm; b) a UV bump between 200 and 260 nm, whose exact position depends upon production conditions and annealing of the samples; the peak is lacking in the as–produced ACH2 sample; c) a decrease in extinction with increasing wavelength from the visual to the mm range, which can be fitted by a power law, $\propto \lambda^{-\gamma}$, with power index γ varying between 1.3 and 0.3, depending on the kind of sample and

spectral sub–interval; d) a number of IR features, mainly due to C–H and C–C resonances.

The results of laboratory experiments evidence that amorphous carbon dust properties vary with the production conditions and/or subsequent processing. The observed differences can be interpreted taking into account variations of a structural parameter, the coherence length, L_a, of the aromatic clusters. This interpretation is supported by the changes measured as a function of thermal annealing of ACH2 samples and going from ACAR to BE samples (see Mennella et al. 1995a,b for more details): the progressive reduction in the hydrogen content, the shift of the UV peak (attributed to $\pi - \pi^*$ electronic transitions) towards 260 nm, the closing of the energy gap, the inversion of the 3.3 μm/3.4μm intensity ratio and the change of the intensity ratio for the so–called "disorder" (at ≈ 1310 cm^{-1}) and "graphite–like" (at ≈ 1590 cm^{-1}) Raman bands. We conclude that, proceding along the thermal annealing of ACH2 grains, i.e. going from ACH2 to ACAR and to BE samples, a growth in the dimensions of sp^2 clusters forming grains occurs which corresponds to a progressive transformation from aliphatic to aromatic character.

Although the previous analogue samples are not duplicates of cosmic dust materials, the physical and chemical parameters which determine their optical behaviour may be relevant also for C–based materials present in space. Therefore, we can expect that the carbonaceous cosmic grains responsible for the UV extinction bump at 220 nm, are less graphitic (i.e. have smaller L_a) than the grains responsible for the 240-250 nm circumstellar bump. Similarly, in the environments where the typical IR C–H stretching features are observed, dominant 3.4–3.5 μm bands indicate an aliphatic character, while a dominant 3.3 μm band suggests a mainly aromatic (i.e. more graphitic) structure of carriers.

Finally, as stressed above, we note that ACAR and BE samples are not obtained by processing the ACH2 sample, but by condensations under different conditions. However, the evolutionary trend as a function of the annealing, mapped by optical and structural properties (such as optical gap and aromatic coherence length; Mennella et al., 1995c), is consistent with the variations in the properties of ACH2, ACAR and BE.

4. Dust heating and IR emission

The temperature of a dust grain at the radial distance r from the exciting star is computed from the balance between grain heating by photon absorption and cooling by photon emission

$$4\langle\varepsilon\rangle\sigma T_d^4 = \int_0^\infty \alpha_\nu \pi B_\nu(T_s) \left(\frac{R_s}{r}\right)^2 \mathrm{e}^{-\tau_\nu(r)} d\nu + \\ + 4\pi \int_0^\infty \alpha_\nu \left(J_{\mathrm{L}_\alpha} + J_{\mathrm{D}} + J_{\mathrm{CL}}\right) d\nu \qquad (8)$$

where

$$\tau_\nu(r) = N_{\mathrm{H}}(r) \left[\sigma_d(\nu) + \sigma_{\mathrm{H}}(\nu) + Y\sigma_{\mathrm{He}}(\nu)\right] \qquad (9)$$

is the total optical depth, α_ν is the absorption cross-section of dust grains, $\langle\varepsilon\rangle$ is the Planck-averaged emissivity for dust grains (Draine and Lee, 1984), σ the Stefan-Boltzman constant, J_{L_α} is the mean intensity of resonantly-scattered Lyman α photons (Tielens and deJong, 1979), J_{D} is the diffuse field (cf Sect. 2), J_{CL} is the field due to cooling line radiation longwards of the Lyman limit. Barlow (1983) showed that the nebular emission escaping from the ionized zone, provide a significant contribution to power the IR emission. Following Middlemass (1990), we included this contribution only in the neutral shell.

The volume emissivity of the dust is

$$\mathscr{J}_\nu(r) = n_{\mathrm{H}}\sigma_{\mathrm{d}}(\nu) B_\nu(T_d) \qquad (10)$$

and the flux at the Earth is obtained by integrating the emissivity over the volume of the nebula

$$F_\nu = \frac{4\pi}{\mathrm{D}^2} \int_{r_c}^{r_{\mathrm{HII}}} \mathscr{J}_\nu(r) r^2 dr \qquad (11)$$

where r_c and r_{HII} are, respectively, the cavity and Strömgren radii and D is the distance of the nebula.

For PNe and evolved HII regions, the nebula is optically thin in the infrared, even with additional dust in the ambient neutral region. In this case, the above treatment can simply be extended to the neutral region. The gas was assumed to extend out to a radius r_{HI}. Close to the external edge r_{HI} of the neutral shell the contribution of the diffuse interstellar radiation field (ISRF) has been included when, depending on model details, the dust temperature drops to the interstellar value. Grain temperatures were computed using the procedure summarized in Eq. (9), and the derived IR fluxes were added to those from the ionized shell.

Heavily-obscured compact HII regions can be optically thick in the near infrared. However, the dust is still optically thin out to the Strömgren radius, so it is possible to evaluate the nebular dust temperatures by means of Eq. (9). Thermal balance in the neutral shell is then solved iteratively, including dust self absorption of infrared radiation.

In the outer parts of extended haloes, the radiation intensity may become so low that very small grains can experience temperature fluctuations.

5. Relevance of laboratory data: the case of NGC 7027

The model region is taken to be ionization bounded, that is, all ionizing photons are absorbed by the nebular gas and dust. If the gas-to-dust ratio for gaseous nebulae is comparable to that for the ISM (i.e. $\mathscr{R} \approx 5 \times 10^{-22}$mag cm^2), then the expected optical depths in the visible are a fraction of unity, depending on the temperature of the exciting star and on the density of the gas. There is also the possibility that dust may be depleted within nebulae; the depletion factor may increase with decreasing distance from the ionizing source, as a result of mechanical destruction and/or evaporation of grains. Since dust infrared emission is essentially independent of kinetic temperature, all model nebulae were computed with a constant electron temperature.

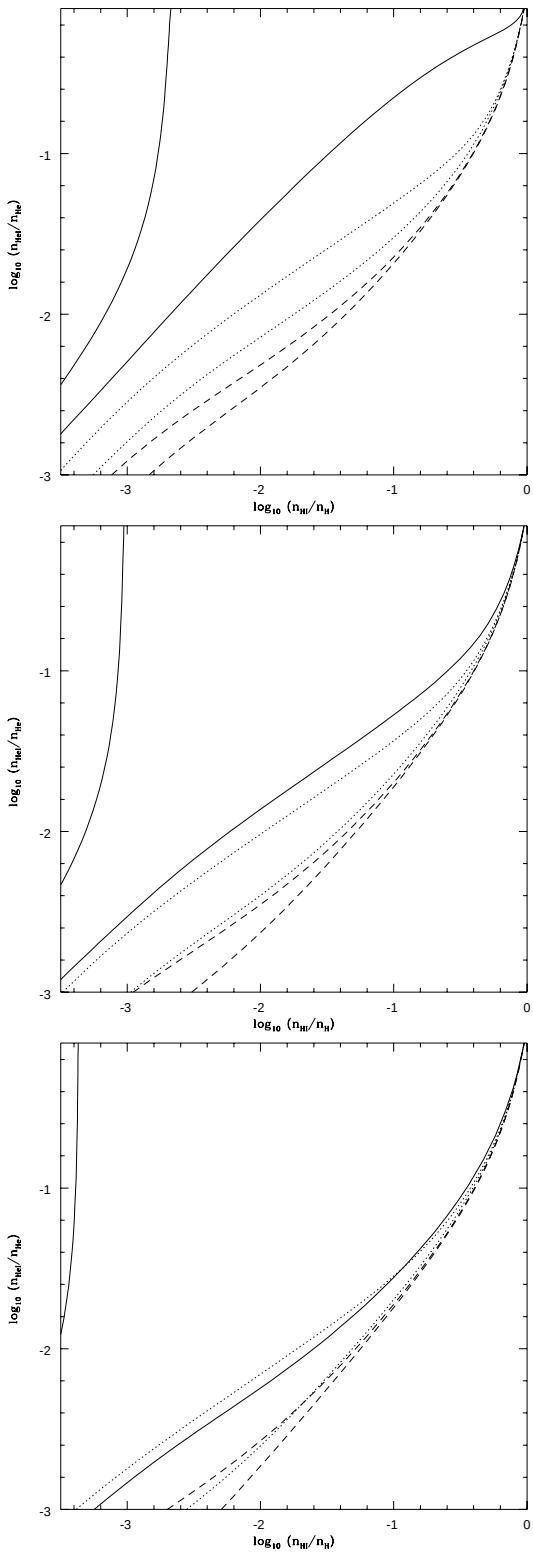

Fig. 1a–c. Ionization boundaries of H and He under different assumptions on radiation temperature: solid line T_s = 35, 000K, dotted line T_s = 50, 000K and dashed line T_s = 75, 000K. Q_H is 10^{48} photons s^{-1}. Thin lines refer to dust-free nebulae, thick lines to dusty environments. **a** n_H=10^3 cm^{-3}; **b** n_H=10^4 cm^{-3}; **c** n_H=10^5 cm^{-3}

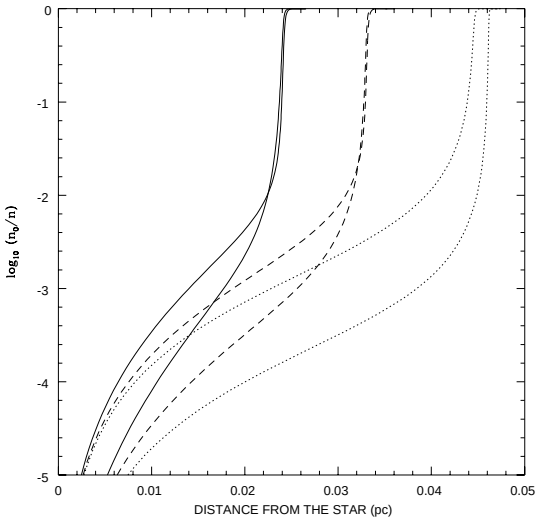

Fig. 2. Ionization structure of a model dusty-nebula (T_s = 35, 000K, Q_H=10^{48} photons s^{-1}, n_H=10^4 cm^{-3}) depending on dust sample choice: solid line ACH2, dotted ACAR and dashed BE. Thin lines refer to the neutral He fraction, thick lines to neutral H fraction

We briefly discuss some results of computations shown in Fig. 1a-c.

As a general trend, dust action tends to merge the ionization boundaries of H and He as a result of the combined effect of strong selective filtering and of the decrease in the ionized volume. However, for $T_s > 50,000$K the ionization structure tends to assume a definite configuration. Dust extinction produces an asimptotic shift towards higher effective radiation temperatures. The He^+/H^+ volume ratio is affected in the case of low stellar temperatures; otherwise, He is ionized throughout the H^+ volume even without the presence of dust. This is in agreement with the results of Aannestadt (1989), who adopted a synthetic dust model.

The use of different dust samples produces large variations in the ionization boundary. These variations reflect different behaviour of the scale of the extinction. ACH2 dust is much more efficient in the extinction of the stellar radiation than ACAR dust. BE dust action is even less important on the location of the ionization front. The lesser hardening of the radiation has the net effect of not coupling the ionization fronts of H and He (Fig. 2).

The temperature of dust grains as a function of the position in the cloud surrounding the central source is shown in Fig. 3 for different dust samples. The drop in dust temperatures at the ionization front is due to the sharp decline in the rate of heating by Lyman α photons. Since in our model the Lyman α flux is proportional to the density of ionized hydrogen, the drop in dust temperatures marks the outer boundary of the ionized zone. The decrease would be, of course, much sharper if the ionized nebula were embedded in a much denser environment, since the occurrence of an "extinction front" screens the external neutral region.

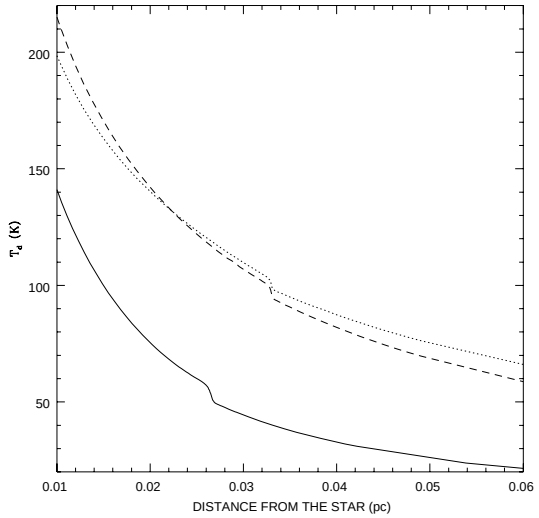

Fig. 3. Dust temperatures in a model nebula defined by T_s = 50, 000K, $Q_H = 10^{48}$ photons s^{-1}, n_H=10^4. Solid line: ACAR; dotted line: BE; dashed line: ACH2

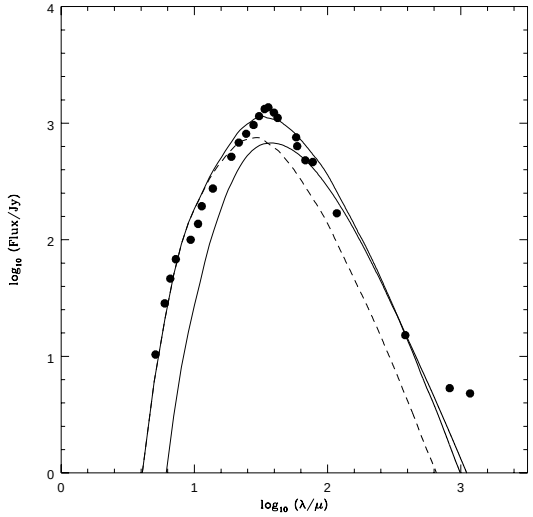

Fig. 4. Model thermal emission from dust grains in NGC 7027. Thick solid line: double shell model with ACAR sample in the ionized region and ACH2 sample in the neutral layer; dashed line: emission from the ionized zone; circles: observations. Thin solid line: model thermal emission with BE sample in the ionized shell and ACH2 in the neutral halo

From the grain temperature it is possible to derive the local dust infrared emission as a function of the distance from the central star. Integration on the nebular volume gives the infrared spectrum from the whole model nebula.

NGC 7027 is very bright in the infrared (Russel et al., 1977; Telesco and Harper, 1977; McCarthy et al., 1978; Aitken et al., 1979; Gee et al., 1984). We used data obtained in the laboratory for the UV to submillimetric ranges to obtain the spectrum of NGC 7027, from 4 to 400 μm. We have not considered here the possibility of reproducing free-free emission from the ionized gas, which dominates continuum emission in the submillimeter range and around 3 μm. Central stars of gaseous nebulae radiate a large amount of ultraviolet radiation during a typical time of 10^3-10^4 yrs. Since UV exposure of carbon grains induces significant changes in the UV-Vis spectrum (Iida et al., 1984; Mennella et al., 1996a), we took into account variations in the physical properties of dust grains. We adopted the optical properties of the ACAR sample in the nebular region, where dust undergoes heavy processing by UV stellar and diffuse radiation. The ionized nebula is surrounded by an expanding molecular cloud which is also assumed to originate from the PN's precursor. In this (relatively) low-excitation, hydrogen-rich environment the optical properties of the hydrogenated amorphous carbon (ACH2 sample) were used. In this scenario ACH2 and ACAR were considered subsequent stages of dust processing (cf Sect. 3). Input model parameters are given in Table 1. The resulting spectrum is shown in Fig. 4, where we also separately show the contribution of the warm and cool dust. The distance of the nebula was taken 1Kpc (cf Middlemass, 1990).

The agreement between computed and observed spectra is remarkable, altough we do not include any modification of the grain size distribution intrinsic to the dust sample. It is well-known that precise fits can readily be obtained by suitable variations in the parameter space. In this work, we have, instead, emphasized the presence of an evolutionary trend that applies to carbon grains. In Fig. 4 we also show the resulting IR emission considering BE dust as the carrier of the intranebular extinction. It is evident that BE dust cannot produce enough near IR emission, due to much lower equilibrium temperatures in the ionized nebula, even enhancing the dust-to-gas ratio. Table 2 gives some information on the dust amount needed to reproduce the observed emission.

Table 1. Input model parameters

T_s (K)	L ($L_\odot$)	N_H (cm^{-3} pc)	τ_V
1.9×10^5	9×10^3	350	0.05

Finally, we estimate the carbon budget needed to reproduce the observed emission. Allowing for the presence of noble gases, we write the mass dust-to-gas ratio as follows

$$\mathscr{R}_M = 4 \times 10^{23} \mathscr{R} k_V^{-1} \quad (12)$$

where k_V is the mass absorption of dust (cm^2 g^{-1}) in the visible. By using the values given in Table 2, we derive C/H=2.4×10^{-5} and 6.3×10^{-5} for ionized and neutral shells, respectively. We note that these results are consistent with new published data on carbon abundance (Snow and Witt, 1995, 1996).

Middlemass (1990) and Hoare et al. (1992) modelled the IR submillimetre observations for NGC 7027, using a photoionization model with a radial-dependent density for dust grains. Our model predicts an intranebular mass of dust of $2 \times 10^{-5} M_\odot$ and a nebular outer radius of about 0.04 pc. The content of dust in the neutral shell is $3.3 \times 10^{-3} M_\odot$. The temperature of

Table 2. Thermal dust emission model

Region	Dust material	H mass ($M_\odot$)	$\mathscr{R}$ (mag cm^2)	$\mathscr{R}_M^{-1}$ Eq. (15)	k_V (cm^2 g^{-1})
HII	ACAR	0.06	5×10^{-23}	3500	7.05×10^4
HI	ACH2	4.30	5×10^{-23}	1300	2.62×10^4

central star is $T_s \approx 1.9 \times 10^5$K. The amount of dust in the ionized shell is consistent with the value obtained by Middlemass (1990) while the mass of dust in the neutral shell is about one order of magnitude larger. Our value is in good agreement with value derived by Hoare at al. (1992) in modelling submillimeter emission. As noted by Hoare et al. (1992) this discrepancy is probably due to an overestimation of the emission line intensities (a factor of 4π) by Middlemass (1990). The outer radius of the nebula obtained by means of our modelling procedure is larger than the Hoare et al. (1992) derivation by about 25%. This is not surprising since we are using a constant density model. In this case, it is probably more meaningful to compare the hydrogen column density (or the visual extinction). We obtained a visual optical depth $\tau_V = 0.05$ that is consistent with a value of 0.06 obtained by Middlemass (1990) at λ5007. A more serious problem is posed by the temperature of the exciting star. Our derived value is probably too large ($T_s \approx 1.4 \times 10^5$, Middlemass, 1990). Correspondingly, there is an over-heating of the dust particles in the ionized shell. We obtained a maximum dust temperature (> 300K) that is somewhat higher than the maximum one derived by Hoare et al. (1992). Our larger values are in agreement with the results of a semiempirical model by Zavagno and Baluteau (1995). This could indicate that classical carbonaceous grains require too high temperatures to provide enough mid-IR emission. We conclude that a population of hot large grains close to the star cannot account for the *total* mid-IR emission. Large molecules (PAHs) and/or very small grains far from the star could significantly contribute to mid-IR spectrum by non-equilibrium emission (Siebenmorgen and Krügel, 1992). However, it is unlikely that non-equilibrium emission by very small particles can dominate the 12-24 μm continuum, since observations show that mid-IR emission is co-extensive with the ionized gas and not extended like the short-wavelength features (Bentley, 1982; Aitken and Roche, 1983). PAHs probably dominate near-IR continuum and band emission. We address these points in the last section.

6. Discussion

Several attempts have been made to identify the actual properties of cosmic dust in the ISM, in circumstellar regions, and in the interplanetary and cometary environments. Many of them have been based on theoretical models, mainly aimed at reproducing the observed spectral characteristics. The main drawback of this approach is that a number of free parameters are often chosen so as to properly reproduce astronomical data, without a careful testing of their plausibility in the context of the galactic evolution.

We have not attempted in this work to provide precise fits for the IR emission of astronomical circumstellar sources. We have shown, instead, that by means of a simple photoionization model which includes UV dust processing, it is possible to account for most of the spectral distribution of dust continuum emission without modifying detailed parameters such as the grain size distribution: we have performed a "physical" rather then a numerical fit. Middlemass (1990) suggested that a mixture of graphite and AC grains could provide a reliable fit to the observed spectrum. On the contrary, the results of the present work give the indication that dust grains respond to environment perturbations modifying their structural properties. There is no need to introduce multimodal dust populations to account for the observed spectrum.

A significant number of gaseous nebulae exhibit the family of unidentified infrared (UIR) bands. The above evolutionary scenario for dust grains in gaseous nebulae should include a description of the emission mechanism and of the carriers of the near-IR emission features. Considerations based on the C/O ratio and its correlation with the luminosity in these features, strongly support the identification of the UIR bands with hydrocarbons associated with carbon grains or PAHs. In particular, evolved PNe show a strong 3.3μm feature and a much weaker 3.4μm feature. On the other hand, the IR spectra of some protoplanetary nebulae show the presence of a strong 3.4μm aliphatic CH band, relative to the usually dominant (in PNe) 3.3μm aromatic feature (Geballe et al., 1992). In two of three dust samples used in this work (ACH2, ACAR), the aliphatic features around 3.4μm dominate the spectrum. On the contrary, the 3.3μm aromatic band prevails in BE sample. In comparison to ACH2 and ACAR grains, BE particles contain larger sp^2 clusters (Colangeli et al., 1995). The 3.3μm emission observed in NGC 7027 (Nagata et al., 1988) could be produced by a thin shell located on the outer edge of internal cavity ($T_d \approx 400$K), where UV processing could have shifted dust internal structure towards more graphitized forms. This suggestion is dismissed on the basis of the observational evidence that in NGC 7027 the 3.3μm is very extended and come exclusively from outside the ionized gas region (Woodward et al., 1993). Recent results on the evolution of the IR spectrum of annealed hydrogenated carbon grains (Mennella et al.,1996b) show that significant changes take place in the IR spectrum of carbon grains because of heat treatment for (relatively) high temperatures. This excludes the occurence of an annealing mechanism far from the exciting star.

A partial contribution to mid-IR emission could come from large molecules and/or small grains located far from the ionized region. In fact, Siebenmorgen and Krügel (1992) present

a good fit of the 1-1000 μm range spectrum of NGC 7027 which includes a substantial contribution from PAHs. However, they could overestimate the overall contribution of all IR emission carriers because of the very high star effective temperature ($T_s = 2.7 \times 10^5$K).

In conclusion, using properties of AC dust and an evolutionary link between dust in the ionized and neutral shells we tried to reproduce the 4-400 μm range continuum emission in NGC 7027. In the mid-IR we partially failed, mostly due to the need of a too high radiation temperature of the central star. Furthermore, we found that it was not possible to reproduce the 3.3μm band emission with hot classical grains, because only the BE sample presents the aromatic feature. In this case the 3.3μm emission carriers would be co-extensive with the ionized gas, contrary to the observations. We conclude that non-equilibrium emission is needed to produce the near-IR bands and part of the underlying continuum. Mid-IR emission is then a superposition of thermal emission from hot AC grains close to the star and non-equilibrium emission far from the ionized gas. Warm AC grains provide the bulk of far-IR and submillimeter continuum emission.

References

Aannestadt P.A., 1989, ApJ, 338, 162.
Aitken D.K., Roche P.F., Spenser P.M., 1979, ApJ, 233, 925.
Aitken D.K., Roche P.F., 1983, MNRAS, 202, 1233.
Barlow M.J., 1983, in *Planetary Nebulae, IAU Symp. No. 103*, 105, ed. D. Flower, Reidel, Dordrecht.
Barlow M.J., 1989, in *Infrared Spectroscopy in Astronomy, Eslab Symp. No. 22*, 307, ed. B.H. Kaldeich, ESA SP-290.
Bentley A.F., 1982, Astr. J., 87, 1810.
Buss R.H., Tielens A.G.G.M., Cohen M., Werner M.W., Bregman J.D., Witteborn F.C., 1993, ApJ, 415, 250.
Colangeli L., Mennella V., Palumbo P., Rotundi A., Bussoletti E., 1995, A&AS, 113, 561.
Colangeli L., Bussoletti E., Cecchi-Pestellini C., Mennella V., Palomba E., Palumbo P., Rotundi A., 1996, Adv. Spa. Res, in press.
Draine B.T., Lee H.M., 1984, Ap. J., 285, 89.
Geballe T.R., Tielens A.G.G.M., Kwock S., Hrivnak B.J., 1992, ApJ, 387, L89.
Gee G., Emerson J.P., Ade P.A.R., Robson E.I., Nolt I.G., 1984, MNRAS, 208, 517.
Harrington J.P., Monk D.J., Clegg R.E.S., 1988, MNRAS, 231,571.
Hoare M.G., 1988, PhD thesis, University of London.
Hoare M.G., Roche P.F., Clegg R.E.S., 1992, MNRAS, 258, 257.
Hummer D.G., Seaton M.J., 1963, MNRAS, 125, 437.
Hummer D.G., Seaton M.J., 1964, MNRAS, 127, 217.
Iida S., Ohtaki T., Seki T., 1984, Am. Inst. Conf. Proc., 120, 258.
Mathis J.S., 1985, ApJ, 291, 247.
McCarthy J.F., Forrest W.J., Houck J.R., 1978, ApJ, 224, 109.
Mennella V., Colangeli L., Blanco A., Bussoletti E., Fonti S., Palumbo P., Mertins H. C., 1995a, ApJ, 444, 288.
Mennella V., Colangeli L., Bussoletti E., Monaco G., Palumbo P., Rotundi A., 1995b, ApJ Supp., 100, 149.
Mennella V., Colangeli L., Bussoletti E., Merluzzi P., Monaco G., Palumbo P. & Rotundi A., 1995c, Planet. Space Sci., 43, 1217.
Mennella V., Colangeli L., Palumbo P., Rotundi A., Schutte W., Bussoletti E., 1996a, ApJ, 464, L191.
Mennella V., Colangeli L., Cecchi-Pestellini C., Palomba E., Palumbo P., Rotundi A., Bussoletti E., 1996b in *From Stardust to Planetesimals*, eds. Y.J. Pendlenton and A.G.G.M. Tielens, in press.
Middlemass D., 1990, MNRAS, 244, 294.
Nagata T., Tokunaga A.T., Sellgren K., Smith R.G., Onaka T., Nakada Y., Sakata A., 1988, ApJ, 326, 157.
Natta A., Panagia N., 1981, ApJ, 248, 189.
Petrosan V., Dana R.A., 1975, ApJ, 196, 733.
Rubin R.H., 1984, ApJ, 287, 653.
Russel R.W., Soifer B.T., Wilner S.P., 1977, ApJ, 217, L140.
Sarazin C.L., 1977, ApJ, 211, 772.
Savage B., Mathis J.S., 1979, ARA&A, 17, 73.
Siebenmorgen R. Krügel E., 1992, A&A, 259,614.
Snow T.P., Witt A.N., 1995, Science, 1455.
Snow T.P., Witt A.N., 1996, ApJ, 468, L65.
Telesco, C.M., Harper, D.A., 1977, ApJ, 211, 475.
Tielens A.G.G.M., de Jong T., 1979, A&A, 75, 326.
Woodward C.E., Pipher J.L., Forrest W.J., Moneti A., Shure M., 1992, ApJ, 385, 567.
Zavagno A., Baluteau J.P., 1995, Planet. Space Sci., 43, 1329.

This article was processed by the author using Springer-Verlag LaTeX A&A style file *L-AA* version 3.